

## Article

# Sustainable Retrofit of Existing Buildings: Impact Assessment of Residual Fluorocarbons through Uncertainty and Sensitivity Analyses

Gianluca Maracchini , Rocco Di Filippo, Rossano Albatici , Oreste S. Bursi and Rosa Di Maggio 

Dipartimento di Ingegneria Civile, Ambientale e Meccanica (DICAM), Università di Trento, 38123 Trento, Italy

\* Correspondence: gianluca.maracchini@unitn.it (G.M.); rosa.dimaggio@unitn.it (R.D.M.)

**Abstract:** Fluorocarbons are an important category of greenhouse gas emissions, and currently, their use is prohibited due to their significant contribution to the global ozone depletion potential (ODP). During this century, they will continue to emit greenhouse gases into the environment since they are present in the thermal insulation foam and HVAC systems in existing buildings; however, proper disposal of these banks of CFCs/HFCs from existing buildings can limit their effects on the environment. However, there are no studies that have investigated quantifying the achievable environmental savings in this case. In this study, a comparative life cycle assessment (LCA) is conducted to evaluate, for the first time in the literature, the environmental savings achievable through the removal and disposal of CFC/HFC banks from buildings including damage-related emissions. To cope with the scarcity of data, uncertainty and sensitivity analysis techniques are applied. The results show that, for the selected archetype building, the largest annual emissions of CFCs/HFCs come from the external thermal insulation of the envelope. The removal of this material can lead to an additional significant reduction in the GWP (up to 569 kgCO<sub>2</sub>eq/m<sup>2</sup>) and the ODP (up to  $117 \times 10^{-3}$  kgCFC-11eq/m<sup>2</sup>), i.e., higher than that achievable by reducing energy consumption through energy retrofit measures (276 and 0, respectively). Thus, CFC/HFC banks should not be neglected in LCA studies of existing buildings due to their possible significant impact on a building's ecoprofile.



**Citation:** Maracchini, G.; Di Filippo, R.; Albatici, R.; Bursi, O.S.; Di Maggio, R. Sustainable Retrofit of Existing Buildings: Impact Assessment of Residual Fluorocarbons through Uncertainty and Sensitivity Analyses. *Energies* **2023**, *16*, 3276. <https://doi.org/10.3390/en16073276>

Academic Editor: Elena Lucchi

Received: 28 February 2023

Revised: 30 March 2023

Accepted: 3 April 2023

Published: 6 April 2023



**Copyright:** © 2023 by the authors. Licensee MDPI, Basel, Switzerland. This article is an open access article distributed under the terms and conditions of the Creative Commons Attribution (CC BY) license (<https://creativecommons.org/licenses/by/4.0/>).

**Keywords:** environmental retrofit; energy retrofit; life cycle assessment (LCA); fluorocarbon; HFC; CFC; uncertainty analysis; sensitivity analysis; natural hazards; performance-based earthquake engineering (PBEE)

## 1. Introduction

The building sector is responsible for 36% of the global energy demand [1] and more than one-third of total global greenhouse gas emissions [2,3]. In addition, energy supply has long become a factor of critical importance for many countries [4]. More precisely, a significant share of building energy consumption in the EU is directly linked to oil and gas, which are mainly imported [5]. Moreover, in 2017, natural gas provided 37% of the district heating in the EU [6], followed by coal with a share of 25%, which comes with significant health and environmental consequences [7]. Consequently, recently, the European Union has put forward several initiatives to promote both energy efficiency and lower environmental impacts in an increasing number of sectors [8–10]. In this regard, growing attention is being paid to the environmental footprint of the building sector [11–14].

Due to the poor energy performance of existing buildings, the main environmental impact is related to building energy consumption for space heating. Therefore, the main actions to reduce the impact of the sector are achieved through energy efficiency measures [15,16]. However, during the building operation stage, other sources of emissions can be observed, which may be potentially relevant in the life cycle assessment (LCA) of a building, despite being generally neglected in common approaches.

One source of emissions is the presence of residual chemicals in building components that have, on the one hand, high environmental impacts (active or passive) which are progressively reintegrated into the environment through different release mechanisms. On the other hand, proper removal and treatment of these substances, when possible, can reduce (or even eliminate) their potential environmental impact, and therefore, can improve the environmental performance of buildings [15,16].

Chlorofluorocarbons (CFCs) and hydrofluorocarbons (HFCs), for example, are substances with high environmental impacts that have been widely used in the past both as blowing agents for thermal insulation and as refrigerants for domestic systems or equipment [17]. Although CFCs are prohibited and HFCs are being phased out, these chemicals are still significantly present within the existing building stock (in the so-called “banks” of CFCs and HFCs), and are gradually emitted into the environment through different release mechanisms [18]. CFCs are characterized by a high global warming potential (GWP) and, above all, a high ozone depletion potential (ODP). To preserve the ozone layer, these substances have been gradually phased out worldwide since 1995, until they were completely banned in 2010 according to the 1989 Montreal Protocol [19,20]. HFCs, which are used as a replacement for CFCs, are characterized by a negligible ODP but a high GWP (although lower than that related to CFCs) [21]. In particular, the contribution of HFCs to global warming, which is still growing globally, is estimated to be around 0.3–0.5 °C by 2100 [22,23]. Therefore, in order to mitigate its effects, the Kigali amendment has provided for them to be phased out over the coming decades [23,24]. However, during the current century, it is expected that CFC/HFC banks will continue to emit up to 5 million tons of CFCs (mainly CFC-11 and CFC-12) [17], equal to 35 billion tons of CO<sub>2</sub>eq, and up to 2 billion tons of CO<sub>2</sub>eq per year for HFCs (before their emissions start to decrease in 2030) [23].

The main emission mechanisms of CFC/HFC banks are known and are mainly related to the release of blowing agents [25,26] and the operational leakages of refrigerants [27,28]. Another emission mechanism is related to structural or non-structural damage caused by extreme events such as earthquakes and hurricanes [18]. In this context, given the high environmental impacts linked to these substances, and considering that several environmental guidelines provide recommendations on their management during disposal to limit or eliminate their environmental impacts [15], the quantification of their extent is of fundamental importance: (i) to correctly estimate the emissions and environmental impacts attributable to the existing building sector [17]; (ii) to assess the possible environmental impacts of extreme natural events such as earthquakes, which may trigger the release of such substances into the environment, as a result of damage to buildings [18,29]; (iii) to estimate the actual environmental savings that can be achieved through environmental retrofit interventions that include, where possible, the correct replacement and disposal of critical building components, e.g., by replacing the thermal insulation coating.

Nonetheless, any quantification of emissions from these mechanisms is complex, as it tends to be influenced by uncertainty, lack of data [17,30,31], and the complexity of the effective emission mechanisms [32]; thus, these issues are still the subject of study and research [17,18]. Therefore, to date, there are very few studies aimed at quantifying and considering such emissions within an LCA of buildings. As an analytical tool, an LCA that included the ODP and the GWP impacts related to emissions of these substances in buildings has recently been presented by Di Filippo et al. [18]. Nonetheless, this study follows a deterministic approach, not considering other existing uncertainties. Moreover, in the literature, there is no application of this tool to a real case study.

In this framework, the aim of this work is twofold: (i) To quantify the reduction in environmental impacts obtainable through the removal of CFC/HFC banks for a case study in Italy; to this end, the analytical tool developed in the aforementioned study by [18] was applied, for the first time, to a real case study, and adequately extended to consider the uncertainties present in the calculation process through sensitivity and uncertainty analysis techniques [11,33,34]. (ii) To compare two different environmental retrofit strategies in

terms of environmental impact. The first retrofit strategy considers the superposition of a new ETICS layer above the existing insulation. The second retrofit, instead of reaching the same thermal performance as in the first strategy, foresees the removal and disposal of the existing ETICS layer and the subsequent addition of a new and thicker ETICS layer.

In summary, the results are aimed at supporting decision-makers and practitioners in the assessment of the environmental convenience of retrofit interventions involving the removal and disposal of CFC/HFC banks from existing buildings.

This paper is structured as follows: In Section 2.1, the phases of the study are briefly summarized. The case study is described in Section 2.2 while the methods used to estimate the expected annual impact due to CFC/HFC banks and to compare the two different environmental strategies are reported in Sections 2.3 and 2.4, respectively. The methodologies adopted for the uncertainty and sensitivity analyses are reported in Section 2.5. Finally, Section 3 reports the results of the study, while the conclusions are presented in Section 4.

## 2. Phases, Materials, and Methods

### 2.1. Phases

This study can be divided into three main phases:

- In the first phase, a building archetype representative of Italian buildings containing CFC/HFC banks is identified and characterized according to the literature in terms of constructive features, thermal characteristics, and energy performance to provide a significant reference study described in Section 2.2.1 [35].
- Then, to evaluate the opportunity of removing and disposing of CFC/HFC banks from buildings as an environmental retrofit strategy, the annual GWP and ODP due to the building CFC/HFC emissions are quantified for the first time in the literature, and then compared with the impacts related to the annual energy consumption for space heating. The methodology developed in [18] is adopted to consider all the release mechanisms, also extending it to consider all the sources of uncertainty in the calculation process (see, in this respect, Sections 3.1 and 3.2).
- Finally, the impact of removing CFC/HFC banks in the life cycle environmental impact of an exemplary retrofit solution is evaluated through the comparison of two iso performance environmental retrofit strategies described in Section 2.2.2, mainly differing from the removal and disposal of CFC/HFC banks before the retrofit intervention described in Section 3.3.

### 2.2. Case Study

#### 2.2.1. Description of the Selected Building

The case study is an archetype, six-story, multi-residential reinforced concrete building placed in the largest climatic zone of Italy (i.e., with heating degree days between 2100 and 3000, referring to a base temperature of 20 °C, zone E [36]) and representative of Italian residential buildings built between 1970 and 2005 [35]. The choice of this archetype as a case study is dictated by: (i) the presence of thermal insulation panels including CFC/HFC banks (polyurethane (PUR), expanded polystyrene (EPS), or extruded polystyrene (XPS) [37,38]) in both the external envelope and intermediate floors; (ii) the presence of an air conditioning (AC) systems for each flat including CFC/HFC banks; (iii) the need to improve the building energy performance according to the current national standards [39]; (iv) the possibility to remove and dispose of the insulation panels from the building envelope (placed as the external thermal insulation composite system (ETICS)), whose profitability as an environmental retrofit strategy is evaluated in this study (see Section 2.2.2).

The building is characterized by a usable floor area of about 545 m<sup>2</sup>, a roof area of 680 m<sup>2</sup>, a vertical opaque surface area of about 2300 m<sup>2</sup>, and a vertical transparent surface area of about 500 m<sup>2</sup>, as described in [35]. The adopted insulation panels have a thermal conductivity of 0.040 W/mK and a thickness of about 0.03 m for vertical and horizontal components [40,41]. From these values, it is possible to approximately estimate the total volume of insulation material included in the building, equal to about 0.06 m<sup>3</sup>/m<sup>2</sup>

of usable floor area, and the volume contained in the external envelope only, equal to about  $0.03 \text{ m}^3/\text{m}^2$ . Concerning the thermal characteristics, the air-to-air thermal transmittance (U-value) of the opaque elements is equal to  $0.63 \text{ W}/\text{m}^2\text{K}$  for brick-cement floors,  $0.57 \text{ W}/\text{m}^2\text{K}$  for roof elements, and  $0.59 \text{ W}/\text{m}^2\text{K}$  for hollow-brick external walls, while the windows have a U-value equal to  $3.3 \text{ W}/\text{m}^2\text{K}$  [35]. The building energy demand is equal to  $70 \text{ kWh}/\text{m}^2\text{y}$  [35]. The heat production system is an autonomous gas boiler for each flat.

Since this study also aims to compute the damage-related environmental impact caused by CFC/HFC emissions (see Section 2.3.3), it is assumed that the building has not already been damaged by seismic events, while two seismic scenarios are considered to evaluate the impact of the seismicity level on the CFC/HFC emissions, i.e., a high-seismic scenario (e.g., L'Aquila, Italy) and a low-seismic scenario (e.g., Trento, Italy), both placed in the climatic zone E [36] and to which thermal characteristics and energy performance are referred.

## 2.2.2. Retrofit Strategies

A typical energy retrofit strategy compliant with national standards [42] is considered in this study [35]. The strategy consists of the application of different measures for the energy upgrading of the building envelope, including (i) the addition of a new ETICS layer on the vertical components to reach a U-value of  $0.25 \text{ W}/\text{m}^2\text{K}$ ; (ii) the addition of a new ETICS layer for the horizontal components to obtain a U-value of  $0.21 \text{ W}/\text{m}^2\text{K}$ ; (iii) the substitution of the existing windows with new ones characterized by a U-value equal to  $1.70 \text{ W}/\text{m}^2\text{K}$ . In this way, the building energy demand is reduced from  $70$  to  $49 \text{ kWh}/\text{m}^2\text{y}$  [35].

Since the aim of this study was to assess the profitability of removing and disposing of CFC/HFC banks as a building environmental retrofit strategy, two alternative approaches for the energy upgrading of the building were considered and compared through a stochastic LCA approach reported in Section 2.4. The first strategy (Solution A) considers the superposition of a new ETICS layer above the existing insulation (Figure 1). The second strategy (Solution B) considers, instead, the removal and disposal of the existing ETICS layer and the subsequent addition of a new ETICS layer (thicker than that in A to reach the same thermal performance as shown in Figure 1). The new ETICS layer is based on the adoption of expanded polystyrene (EPS) for the thermal insulation material since it is the most adopted solution in engineering practice [41,43].

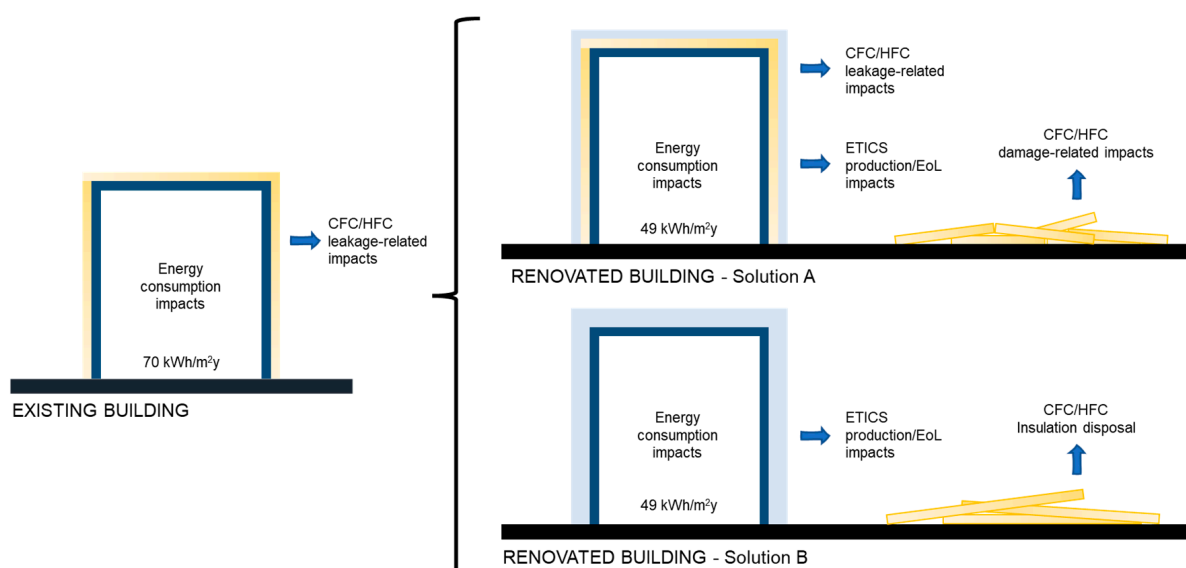


**Figure 1.** Alternative energy retrofit solutions for the building envelope and related emissions. Solution A: superposition of a new ETICS layer above the existing ETICS layer. Solution B: removal and disposal of the existing ETICS layer and the subsequent addition of a new layer.



### 2.3. CFC/HFC Expected Annual Impact

CFCs and HFCs can be present in buildings as blowing agents of insulation materials [38] and as a refrigerant within AC systems [44]. These components typically have a service life of several decades or, in any case, equal to the estimated service life of the buildings, during which they can emit CFCs/HFCs in the environment through different release mechanisms. The estimation of the residual content of CFC/HFC banks in buildings and their annual emissions is then essential for a correct LCA of an existing building [37].

In this subsection, the methodologies adopted to estimate the theoretical residual contents of CFC/HFC banks and the related annual emissions and environmental impacts are reported. Since a stochastic approach is considered (see Section 2.5), in the following, all the uncertain parameters involved in the calculation process will be defined in terms of probability density function (PDF) rather than with deterministic values (mainly uniform PDFs).

#### 2.3.1. Initial Theoretical Size of CFC/HFC Banks

The expected theoretical contents of CFC/HFC within insulation materials per usable area ( $C_I$ ) can be computed as follows:

$$C_I = 0.9 \cdot v \cdot \rho \cdot c_I \quad (1)$$

where 0.9 is a reduction coefficient that considers the amounts of CFCs/HFCs released during the insulation manufacturing and first year of installation (about 10% according to [37]),  $v$  is the volume of insulating material (in  $\text{m}^3/\text{m}^2$  of usable area),  $\rho$  is the density of the insulating material, and  $c_I$  is the content of CFC/HFC expressed in terms of percentage of insulation weight. In this study,  $\rho$  is not known. Hence, a variation between 25 and 55  $\text{kg}/\text{m}^3$  is assumed according to the literature [40,41], thus neglecting the influence of the density on the actual thermal transmittance [40,41]. Concerning  $c_I$ , a range of variation between 7 and 19% is considered according to estimations from multiple sources. In detail, [45] reported a range from 7.4 to 16.9%, [46] a value of 10% and [47] a range from 6.4 to 19.5%.

To calculate the amount of refrigerant gas contained in AC systems, the presence of a double split for each residential unit is considered, given its spread use in the international housing stock. The theoretical content of the refrigerant in the AC system per  $\text{m}^2$  of usable area ( $C_{AC}$ ) can be computed as follows:

$$C_{AC} = r_{AC} \cdot P_{AC} \quad (2)$$

where  $r_{AC}$  is the average refrigerant charge of the system, generally ranging between 0.24 and 1  $\text{kg}/\text{kW}$  [44], while  $P_{AC}$  is the system capacity, which is assumed to range between 0.063, as in [18], and 0.1  $\text{kW}/\text{m}^2$ , as in [48,49]. It should be noted that this calculation neglects the type of refrigerant used. However, as highlighted in [50], the charge size for CFCs and old-generation HFCs does not vary significantly for small equipment (i.e., up to a capacity of 88 kW).

#### 2.3.2. Operational Leakage and Actual Content

The most important CFC/HFC emissions during the life of a building are due to operational leakage. In particular, for insulating materials, the yearly leakage rate ( $l_i$ ) depends on the type of application and insulation material [32]. This rate can vary from 0.25% to 2.5% according to [37] and from less than 0.5% to 1% according to [38]. In this study, we assumed a range from 0.25% to 2.5%. For AC systems, the leakage rate ( $l_{AC}$ ) depends on the type of system, typically 0.1% per year for modern “leak-tight” domestic applications [51] (as the case study here considered) and 10% for commercial systems [51,52]. In this study, a variation of 10% to 0.1% is assumed for  $l_{AC}$ .

As a result of the operational leakage, the actual, residual contents of CFCs/HFCs in buildings may be different from its initial content. Indeed, the residual content may

vary with the age of installation, operating history, and level of maintenance of the systems. Accordingly, the residual contents of CFCs/HFCs ( $R_y$ ) can be estimated as follows:

$$R_y = (1 - l_y \cdot t_y) \cdot C_y \quad (3)$$

where  $t$  is the age in years of the specific emission source “ $y$ ”, i.e., insulation ( $I$ ) or AC. To evaluate the impact of this parameter on the results, in this study, we assumed that the ages of the insulation ( $t_I$ ) and AC system ( $t_{AC}$ ) could vary between 15 and 30 years, coherently with the assumed construction period.

### 2.3.3. Analytical Framework for Damage-Related Leakage

To integrate methods for calculating the environmental impact of natural disasters on structures that rely solely on metrics derived from or similar to embodied carbon [53], this study used the content release GHG emission potential (CGEP) framework, which was originally developed for the assessment of greenhouse gas emissions from Natech incidents [29], and then extended to the content release ODP emission potential (CODP) and residential structures [16].

This method considers the emissions of high GWP and ODP chemicals into the environment, including the class of fluorocarbons. Based on the analysis of the effects of the 2011 Tohoku earthquake, it has been shown that this class of emissions is comparable to those from repair, reconstruction, and debris disposal operations [54,55]. The CGEP framework consists of 4 distinct phases:

1. Evaluation of the CGEP and CODP parameters of the structure/component under examination through the estimation of the contents of high GWP and/or ODP compounds;
2. Assessment of the probability  $P_{fn}$  of a certain failure state induced by the natural hazard  $n$ ;
3. Assessment of the fractions of CGEP and CODP,  $RL_{fn}$  released in the environment following the damage state related to  $P_{fn}$ ;
4. Calculation of the expected emissions  $EM_n$  due to the above-mentioned release.

While the framework can be applied to various types of natural hazards, in this study, the analysis focuses solely on seismic events. In addition, the high GWP and ODP chemicals used for the calculation of the CGEP and the CODP are the fluorocarbons, including HFCs and CFCs, that are present in the typical building structure. The specific content and the relevant parameters from Step 1 have already been calculated in Sections 2.3.1 and 2.3.2.

Subsequently, to assess the probability of failure for a specific structure or component, Phase 2 involves a process known as a quantitative risk analysis (QRA). This analysis can be performed using the PBEE framework [56,57] or by utilizing specific databases, statistical data, or the results from other studies. The mathematical formulation of  $P_{fn}$ , can be expressed as follows:

$$P_{fn} = \int_{IM_n} P(DM_f | IM_n) d\lambda(IM_n) \quad (4)$$

The subscript  $f$  is used to indicate the particular type of failure associated with a certain capacity damage state  $DM_f$ , while the variable  $n$  represents the selected natural hazard, which can be an earthquake, flood, tsunami, or other events. The parameter  $d\lambda(IM_n)$  describes the hazard level in terms of a specific intensity measure  $IM$ . The proportion of content release is observed to vary according to different damage levels. Thus, in Phase 3 of the process, it is essential to assess this proportion as follows:

$$RL_f = \frac{CGE_f(DM_f)}{CGEP} = \frac{COE_f(DM_f)}{CODP} \quad (5)$$

where  $CGE_f(DM_f)$  and  $COE_f(DM_f)$  are the fractions of CGEP and CODP effectively released in the environment following the damage state  $DM_f$ . For simplicity, the two variables

will be assumed to be equal for each chemical compound considered. Phase 4 ultimately combines the results from the other 3 phases to calculate the annual emissions resulting from the considered hazards and associated damage states as follows:

$$EM_n = P_{fn} \cdot RL_f \cdot CGEP \quad (6)$$

Indeed, the expected emissions  $EM_n$  could also be the result of different damage states  $DM_f$  and different natural hazards  $n$ . It should be emphasized that this quantity of emissions should not be considered to be issued annually but represents, to use an economic term, the annual amortization of the impact of the seismic events considered, of which it is not possible to predict the period of occurrence but only its probability.

#### 2.3.4. CFC/HFC Characterization Factors

After quantifying the annual emissions of CFC/HFCs, the associated GWP and ODP can be computed by multiplying these quantities by the related characterization factors. To do so, the quantity of CFC and HFC in each element should be estimated. In this study, as in [18], two different scenarios are assumed which consider, respectively, the content of only CFC (S1) and only HFC (S2) within the building. Assuming that the CFC is an R11 and the HFC is an R134a, the characterization factors for these substances are known, namely  $ODP_{S1} = 1$  and  $GWP_{S1} = 4660$  for S1 and  $ODP_{S2} = 0$  and  $GWP_{S2} = 1300$  for S2 [21].

#### 2.4. LCA of the Sustainable Retrofit Strategies

In this study, two stochastic LCAs were performed at the building level, based on the procedures defined in ISO 14040, ISO 14044, EN 15804, and EN 15978 standards [58–61].

##### 2.4.1. Goal and Scope Definition

The goal of the LCA study was to compare the environmental impact of two different energy retrofit measures for energy upgrading of the building envelope described in Section 2.2 (Solutions A and B, see Figure 1). Then, the reference flow was related to a functional unit (FU) defined as “the energy retrofit measure required to reach the same thermal transmittance of the building envelope [ $W/m^2K$ ], for a reference study period expressed in years”. In particular, Solution A considers the possible addition of an ETICS layer above the existing layer to reach the national requirements in terms of thermal transmittance of the opaque envelope (Figure 1, Solution A). Solution B, instead, first considers the removal and disposal of the existing insulation to eliminate the potential impact of CFC/HFC during the life cycle of the building. Then, a new ETICS layer is added to reach the same thermal performance (Figure 1, Solution B). As a result, in Solution B, a thicker new insulation layer is applied, leading to a higher impact in the production stage as well as in the construction/removal process (due to the CFC/HFC emissions generated during the removal of existing ETICS layer), but to lower emissions of CFCs/HFCs during the operational stage (no operational leakage or damage-related emissions).

Since this is a comparative study, only the relevant LCA stages differing in Solutions A and B are evaluated for the sake of conciseness [61]. In particular, the considered stages are: (i) the production stage (Modules A1–A3 according to [61]), considering the impacts of the different materials only (i.e., insulation layer); (ii) the removal process of the existing insulation (Module A5, for Solution B only); (iii) the use stage (Modules B1 and B6); (iv) the end-of-life (EoL) stage (Modules C1–C4), for the insulation material only as produced in Modules A1–A3. Concerning the use stage, the emissions due to CFC/HFC banks during the use stage (Module B1) are considered, while the impacts related to energy consumption for space heating (Module B6) are computed to be used as a reference quantity to which all other stages are related. Other impacts (e.g., those related to the removal or installation of existing or new ETICS layers, the disposal of the existing layer, maintenance and repair, etc.) are not considered, since they are shared by the two solutions (i.e., all the materials are considered to be installed, removed, and disposed of similarly during or at the end of the building service life). Concerning the removal of the existing insulation for Solution

B (Module A5), this is assumed to be 10% of the  $R_I$ , i.e., equal to the CFC/HFC leakage during the manufacturing and first year of installation [37].

Finally, a calculation period of 50 years is considered, assumed to correspond to the service life of the two retrofit interventions.

#### 2.4.2. Life Cycle Impact Assessment (LCIA) and Life Cycle Inventory (LCI)

Concerning the LCIA, in this study, the CML-2001 baseline V3.02/EU25 method [62] was adopted to calculate the GWP and the ODP of the two solutions, since it is widely applied in the building sector [63,64]. The inventory data were collected from different sources, i.e., the environmental product declarations (EPDs) of the materials (A1–A3 modules), scientific literature (B1 and A5 modules), and generic databases such as ecoinvent [65] (C1–C4 and B6 modules).

For the production phase, the data related to the A1–A3 impacts of the new insulation layer (EPS) were derived from the EPDs collected in [41]. These data are related to a reference flow of mass per square meter providing an additional R equal to 1 m<sup>2</sup>K/W and can be described by using a normal PDF with an average value ( $\mu$ ) of 2.62 kgCO<sub>2</sub>eq/m<sup>2</sup> and a standard deviation ( $\sigma$ ) of about 0.67 kgCO<sub>2</sub>eq/m<sup>2</sup>.

Concerning B1, the characterization factors, as reported in Section 2.3.4, were adopted. On this basis, two different scenarios were assumed, which considered, respectively, the contents of only CFC (S1) and only HFC (S2). As a result, four different scenarios were considered, two for each retrofit solution, namely A-1, A-2, B-1, and B-2.

For B6 and C1–C4, the datasets included in the ecoinvent v3.1 database were adopted to create the relevant PDFs. These are the “Heat, central or small-scale, natural gas IT | heat production, natural gas, at boiler modulating < 100 kW | Alloc Rec, U” and “Municipal solid waste (waste scenario) {RoW} | Treatment of municipal solid waste, landfill | Alloc Rec, U” for B6 and C1–C4, respectively [65]. The characteristics of the PDFs are reported in [33,34] and Table 1.

**Table 1.** Characteristics of the considered PDFs. \* For uniform distribution, min and max; for normal distributions,  $\mu$  and  $\sigma$ ; for lognormal distributions,  $\mu_{\log}$  and  $\sigma_{\log}$ .

Parameter (Unit)	Description	PDF Type	PDF Parameters *
$r_{AC}$ (kg/kW)	Refrigerant charge of AC system	Uniform	0.24, 1.00
$P_{AC}$ (kW/m <sub>2</sub> )	Power of AC system	Uniform	0.063, 0.100
$\rho$ (kg/m <sup>3</sup> )	Density of the insulating material (PUR)	Uniform	25, 55
$c_I$ (%)	Percentage of CFC/HFC of the weight of the insulating material	Uniform	7, 19
$l_{AC}$ (%/year)	Annual operating leakage rate in AC systems	Uniform	0.09, 0.11
$l_I$ (%/year)	Annual operating leakage rate in insulation materials	Uniform	0.25, 2.5
$t_I$ and $t_{AC}$ (years)	Age of insulation/ AC	Uniform	15, 30
$s$ (%)	Annual leakage due to seismic events	Uniform	0, 0.13
GWP <sub>HP</sub> (kgCO <sub>2</sub> eq/kWh)	GWP for gas boilers heat production	Lognormal	−1.34, 0.17
ODP <sub>HP</sub> (kgCFC-11eq/kWh)	ODP for gas boilers heat production	Normal	$3.31 \times 10^{-9}$ , $0.68 \times 10^{-9}$
GWP <sub>A1–A3</sub>	GWP for EPS insulation material production	Normal	2.62, 0.67
GWP <sub>C1–C4</sub>	GWP for EPS insulation material EoL	Lognormal	−2.31, 0.46

## 2.5. Uncertainty and Sensitivity Analysis

The ISO 14044 standard [59] for an LCA defines uncertainty analysis as a systematic procedure to quantify the uncertainty introduced in the results. In this study, uncertainty analysis (UA) and sensitivity analysis (SA) methods were used to better understand the obtained outcomes and to increase the reliability, confidence, robustness, and applicability of the results given the high uncertainties of input data [66,67]. In particular, a quasi-random Monte Carlo (MC) approach based on Sobol's sequence sampling technique was adopted to propagate the uncertainties into the output distribution (UA) and to decompose the output variance on the input parameter uncertainty, identifying the most influential parameters' uncertainty on the output variance (SA) [66,67]. Sobol's sampling method was chosen due to its ability to cover the domain more uniformly than other techniques and to efficiently perform global SA methods. Because they can provide more information about the effect of various inputs on the output, in fact, global SA methods are generally considered to be more accurate than local methods.

These methods require the definition of the PDFs of all uncertain input variables based on the available information, as already presented in the previous subsections (see Sections 2.3 and 2.4). In Table 1, the characteristics of the PDFs adopted in this study are reported. In particular, where no information about the distribution shape could be retrieved, a uniform distribution was adopted.

The results of the UA can be represented through probability density functions (PDFs), cumulative distribution functions (CDF), and/or box-whisker plots of the output samples. Instead, the main outcomes of the Sobol' SA are the first-order ( $S_1$ ) and total-order ( $S_T$ ) sensitivity indexes of the input variables. The  $S_1$  sensitivity index measures the main effect of the input variable on the output and indicates how much the output variance could be reduced if the parameter was fixed. The  $S_T$  sensitivity index, instead, considers both  $S_1$  sensitivity index along with the effect of the interaction of that input parameter with others.

The number of simulations required for the SA, in the case where both the  $S_1$  and  $S_T$  sensitivity indexes are calculated, is equal to  $2N(1 + D)$ , where  $D$  is the number of input variables and  $N$  is a value that is increased until a convergence of the  $S_T$  values is reached [66,67]. In this study,  $D$  is equal to 8 for computing the CFC/HFC annual expected emissions (see Sections 3.1 and 3.2) and  $D$  is equal to 9 to compute the impacts of the alternative strategies (see Section 3.3). Concerning  $N$ , a convergence analysis is carried out in both cases, obtaining an  $N$  value of 1024. The number of simulations is equal to 18,432 and 2048, respectively. Then, the output samples are used for the UA.

## 3. Results and Discussion

### 3.1. CFC/HFC Annual Expected Emissions

#### 3.1.1. Theoretical Content and Source Comparison

The theoretical contents of CFC/HFC due to insulation ( $C_I$ ) and AC systems ( $C_{AC}$ ) are quantified herein for the selected case study. Figure 2 shows the results of the UA in terms of PDFs, CDFs, and box-whisker plots. In addition, the median, mean ( $\mu$ ), mode, standard deviation ( $\sigma$ ), and coefficient of variation (CoV) are also reported for each sample.

In particular,  $C_I$  and  $C_{AC}$  have  $\mu$  values of 281 and 50 g/m<sup>2</sup>, respectively, with  $\sigma$  equal to 98 and 19 g/m<sup>2</sup>, corresponding to CoVs of 35 and 38%, respectively. These data show that  $C_I$  has the largest bank of CFCs/HFCs for the considered case study (on average 5.6 times higher than  $C_{AC}$ ). The obtained result differs from those achieved in previous works, where, instead, the AC systems were the main CFC/HFC banks [18]. This difference is, however, attributable to the different amounts of insulation considered in this study, calculated for a specific building rather than as an average for the entire residential buildings stock (as considered in [18] based on data from a California, USA, inventory). Moreover, this difference was expected because of the significant mass of thermal insulation and the long banking period of foaming agents [37]. While many of the data sources used here are based on empirical or experimental data, an ex-post large-scale validation of these contents is difficult to achieve. The only existing tentative data source in



this direction was developed by [18], in which theoretical estimations were compared with empirical results from atmospheric concentrations after the 2011 Tohoku earthquake [54]. The comparison, however, has proven the accuracy, within one order of magnitude, of the theoretical estimation.

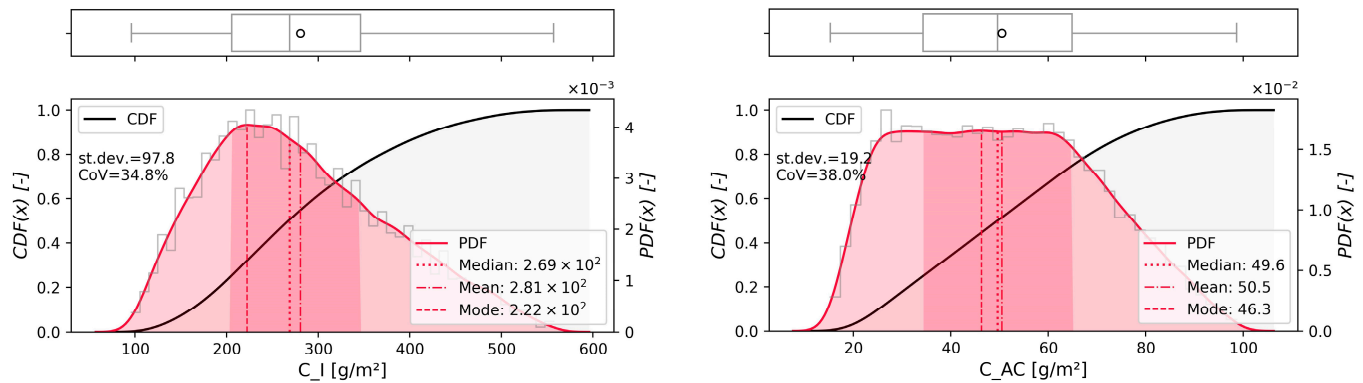


**Figure 2.** PDFs, CDFs, and box-whisker plots for  $C_I$  and  $C_{AC}$ .

### 3.1.2. Operational Leakage and Actual Content

The output samples related to the annual operating leakage from insulating materials ( $L_I$ ) and AC systems ( $L_{AC}$ ) are reported in Figure 3a,b, respectively. As expected, according to the higher annual leakage rate ( $L_I$ , see Table 1) and greater amounts of CFCs/HFCs within the insulation materials ( $C_I$ , see Figure 2), the  $L_I$  is greater than  $L_{AC}$  by two orders of magnitude. In particular,  $L_I$  and  $L_{AC}$  are characterized by  $\mu$  values of 3.43 and 0.05 g/m<sup>2</sup> and CoVs equal to 61 and 39%, respectively.

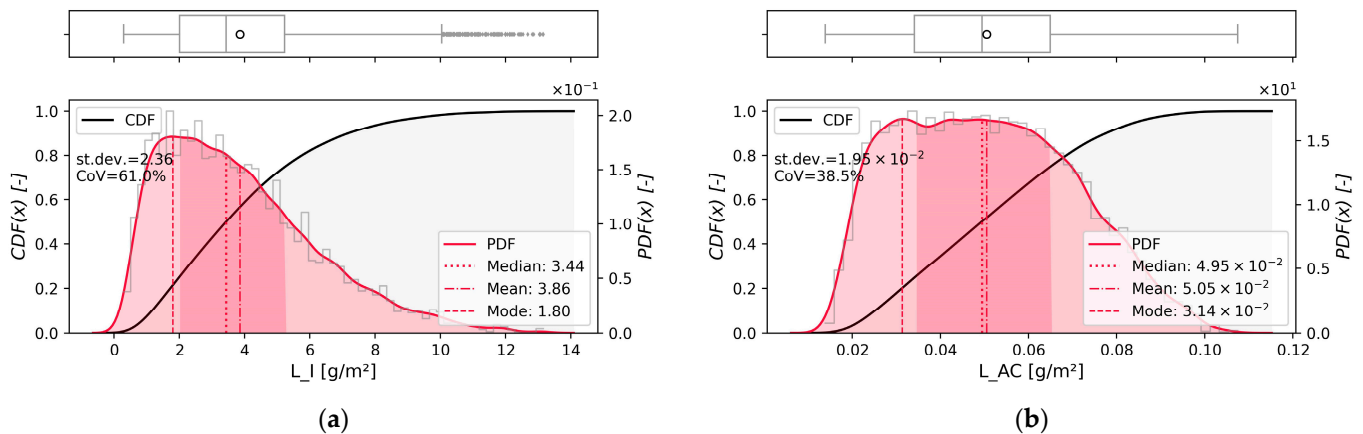


**Figure 3.** PDFs, CDFs, and box-whisker plots for  $L_I$  (a) and  $L_{AC}$  (b).

The PDFs of the residual contents of CFCs/HFCs from insulating materials ( $R_I$ ) and AC systems ( $R_{AC}$ ) are reported in Figure 4. Clearly, as expected,  $R_I$  remains significantly higher than  $R_{AC}$ , as seen for  $C_I$  and  $C_{AC}$  in Figure 2 with  $\mu$  equal to 180 and 50 g/m<sup>2</sup>, respectively. Comparing these quantities with those related to the initial contents ( $C_I$  and  $C_{AC}$ , Figure 2), it can be noted that the installation time of the insulation system ( $t_i$ ) has a significant impact on  $R_I$  due to the high leakage rate  $L_I$ . Conversely, deviation from the initial content is quite null for the AC system, mainly due to the limited annual emissions  $L_{AC}$ . In any case, the residual content seems not to reach zero values, indicating that, even 30 years after their installation, both the insulation material and AC systems can still contain a significant amount of CFC/HFC banks.

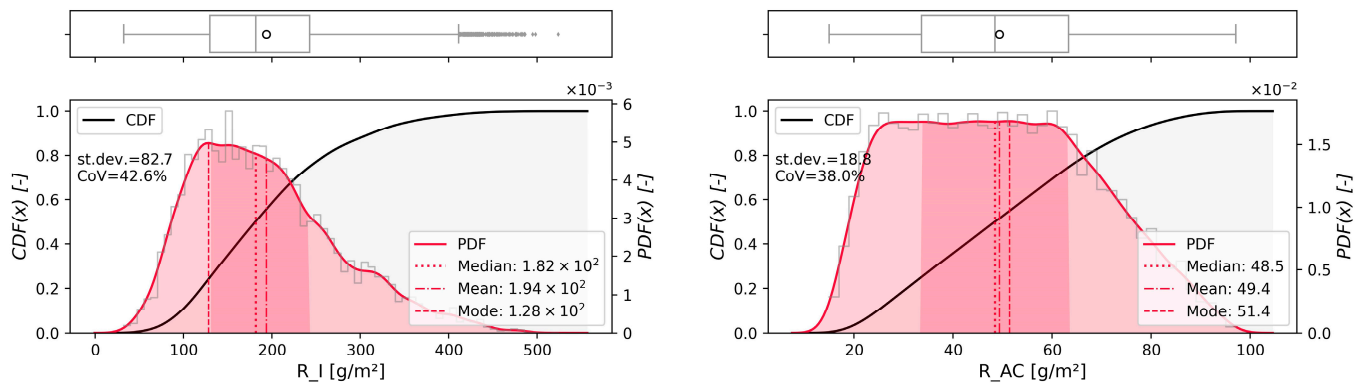


**Figure 4.** PDFs, CDFs, and box-whisker plots for  $R_I$  and  $R_{AC}$ .

### 3.1.3. Assessment of Damage-Related Emissions

The method used here for the calculation of CFC/HFC releases due to seismic events is based on the PBEE approach [30,31] that assumes seismic hazard, seismic vulnerability, damage states, and relevant consequences as statistically independent, and then combines them to estimate the average annual expected loss. Equation (7) requires the definition of a hazard model  $\lambda(IM_n)$  and a probabilistic relationship between a certain damage state and the intensity measure, i.e.,  $P(DM_f | IM_n)$ . In the case study presented here, the seismic hazard was obtained from INGV [68] data, for the municipality of L'Aquila and Trento (Italy), as shown in Figure 5, assumed as representative of a high and low seismicity scenario. In addition, fragility functions were used to characterize the probability of damage states. The analytical formulation of such a function can be expressed as follows:

$$F_{Rd} = P(IM = im) = \phi \left[ \frac{\ln(im/m_d)}{\beta_d} \right] \quad (7)$$

where  $\phi$  indicates a lognormal cumulative distribution function, while  $m_d$  and  $\beta_d$  are the median and the dispersion of the distribution, respectively. To characterize the seismic vulnerability, the parameters of the fragility curves obtained from empirical data were used [47]. In particular, reference was made to high-rise reinforced concrete buildings, i.e., characterized by more than four floors, and built with pre-1981 and post-1981 seismic designs. Therefore, structures with a design based solely on gravity loads were excluded. Furthermore, the first four damage states (DS1, DS2, DS3, and DS4), deriving from the EMS-98 macroseismic model, were considered to be in agreement with [9] which excluded the damage state of structural collapse DS5. This is because the components under consideration, i.e., the infill walls and AC components, can be classified as non-structural and completely damaged already in the penultimate state of damage. The parameters of the lognormal functions of seismic fragility are reported in Table 2.

We also assume that  $RL_{DS4}$  and  $RL_{DS3}$  are equal to 1 and 0.5, respectively [9]. Instead,  $RL_{DS2}$  and  $RL_{DS1}$  are equal to 0.1 and 0.02 in agreement with the estimate of the damages as a fraction of the initial costs reported in [48]. It should be emphasized that, unlike the higher damage states, the less important ones realistically only damage the non-structural components, which, by themselves, represent the major fraction of the construction costs. Combining the hazard, vulnerability, and RL data as per the CGEP framework [9], it is possible to obtain the emission values for each damage state. The results and parameters of the framework are shown in Tables 3 and 4 for L'Aquila and Trento, respectively.

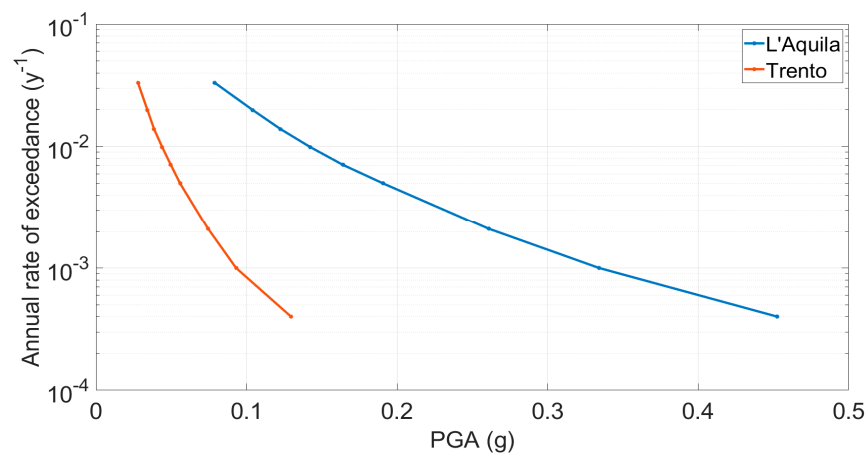


**Figure 5.** Seismic hazard curves of L'Aquila and Trento, Italy. PGA, peak ground acceleration.

**Table 2.** Seismic fragility function parameters.

Type of RC Building	Median $m_d$ (g)				Dispersion $\beta_d$
	DS1	DS1	DS3	DS4	
High rise pre-1981	0.183	0.306	0.423	0.687	0.499
High rise post-1981	0.186	0.351	0.598	1.129	0.531

**Table 3.** Content fractions to be emitted each year due to seismic risk for each damage state and other CGEP framework parameters for L'Aquila.

Damage State	$RL_{DS4}$	Probability (year <sup>-1</sup> )		Fraction Released (%/year)	
		Pre-1981	Post-1981	Pre-1981	Post-1981
DS1	0.02	$1.10 \times 10^{-2}$	$1.37 \times 10^{-2}$	$2.2 \times 10^{-2}$	$2.74 \times 10^{-2}$
DS2	0.1	$4.30 \times 10^{-3}$	$3.40 \times 10^{-3}$	$4.3 \times 10^{-2}$	$3.4 \times 10^{-2}$
DS3	0.5	$1.70 \times 10^{-3}$	$4.87 \times 10^{-4}$	$8.5 \times 10^{-2}$	$2.44 \times 10^{-2}$
DS4	1	$2.09 \times 10^{-4}$	$8.03 \times 10^{-6}$	$2.09 \times 10^{-2}$	$8.03 \times 10^{-4}$

**Table 4.** Content fractions to be emitted each year due to seismic risk for each damage state and other CGEP framework parameters for Trento.

Damage State	$RL_{DS4}$	Probability (year <sup>-1</sup> )		Fraction Released (%/year)	
		Pre-1981	Post-1981	Pre-1981	Post-1981
DS1	0.02	$4.37 \times 10^{-4}$	$6.75 \times 10^{-4}$	$8.74 \times 10^{-4}$	$1.35 \times 10^{-3}$
DS2	0.1	$2.15 \times 10^{-5}$	$9.46 \times 10^{-6}$	$2.15 \times 10^{-4}$	$9.46 \times 10^{-5}$
DS3	0.5	$1.36 \times 10^{-6}$	$1.78 \times 10^{-8}$	$6.53 \times 10^{-5}$	$8.9 \times 10^{-7}$
DS4	1	$1.55 \times 10^{-9}$	$2.96 \times 10^{-14}$	$1.55 \times 10^{-7}$	$1.55 \times 10^{-12}$

However, the values reported in Tables 3 and 4 must be combined by considering the hierarchical scale of the damage states [9]. It follows that, for a building placed in a high seismicity scenario (L'Aquila, Italy), the total content fractions emitted annually due to seismic risk (s) are equal to 0.13% and 0.07% of  $R_I$  and  $R_{AC}$  for the pre-1981 and post-1981 buildings, respectively. Conversely, for a low seismicity scenario (e.g., Trento, Italy) the maximum value is in the order of 0.001%. Then, a range of variation from 0 to 0.13% is considered to evaluate the impact of the seismicity on the results.

According to these quantities, Figure 6 reports the amounts of CFCs/HFCs emitted annually due to seismic risk due to insulation material ( $S_I$ ) and AC ( $S_{AC}$ ). In particular,  $S_I$  and  $S_{AC}$  have  $\mu$  values of 0.13 and 0.03 g/m<sup>2</sup>, respectively, with very high CoVs of 76 and

73%. If a comparison with the operational leakage is made ( $L_I$  and  $L_{AC}$  in Figure 3), it can be observed that, while  $S_{AC}$  shares the same order of magnitude with  $L_{AC}$ ,  $S_I$  is, instead, an order of magnitude lower than  $L_I$ . Then, considering the probability of occurrence of seismic events, the damage-related emissions, in terms of yearly amortization, can be considered to be negligible, in probabilistic terms, with respect to other release mechanisms.

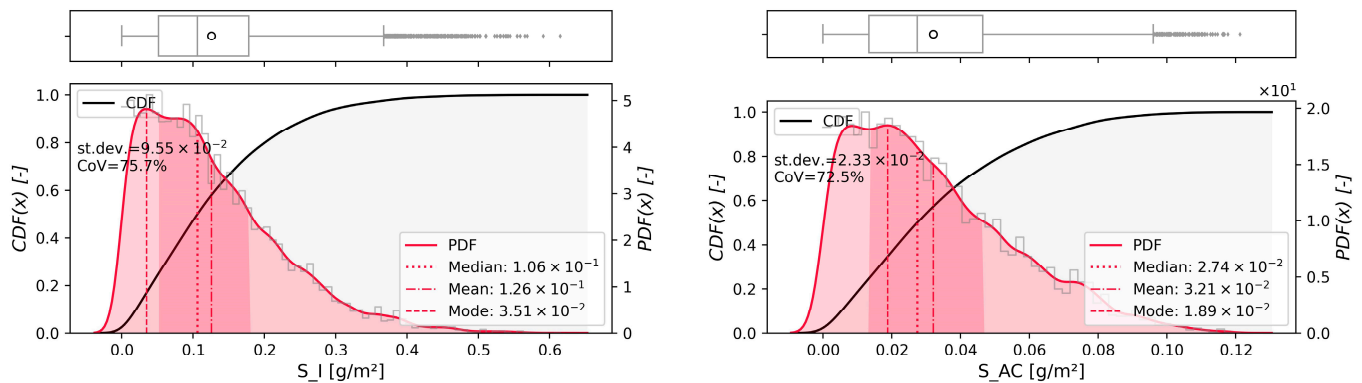


**Figure 6.** PDFs, CDFs, and box-whisker plots of  $S_I$  and  $S_{AC}$ .

### 3.2. CFCs/HFCs Annual Expected Impact

#### 3.2.1. Environmental Annual Impact Due to Heat Production

Before calculating the annual expected impact due to CFCs and HFCs, the annual environmental impact due to heat production is computed in order to provide a reference value to be compared with the annual expected impact due to CFC/HFC emissions. Figure 7a,b show the annual expected impacts obtained in terms of GWP and ODP, respectively. In particular, these impacts are characterized by quasi-Gaussian probability distributions with a limited uncertainty (CoVs equal to 17.1 and 20.5%, for the GWP and the ODP, respectively, caused by the uncertainty of the selected ecoinvent dataset), and average values in line with those reported in the literature [13], equal to  $18.6 \text{ kgCO}_2\text{eq/m}^2$  and  $2.3 \times 10^{-7} \text{ kgCFC-11eq/m}^2$ .

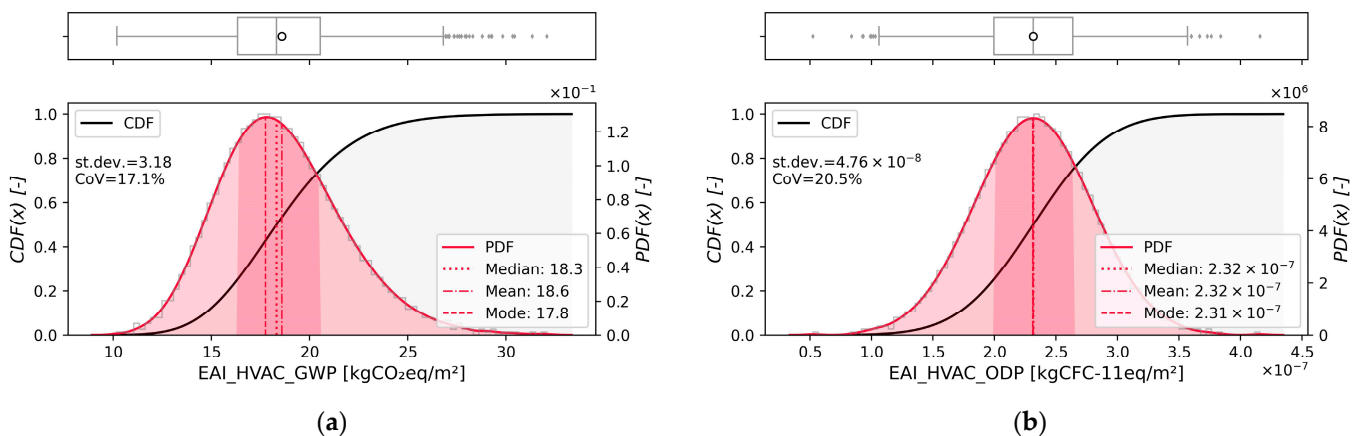


**Figure 7.** PDFs, CDFs, and box-whisker plots for: (a) GWP and (b) ODP due to annual building energy consumption for space heating.

#### 3.2.2. Total Potential Impacts of CFC/HFC Banks

In Figure 8, the potential impacts due to the total residual content  $R_{tot}$  are shown. The results are reported for both scenarios, i.e., S1 (Figure 8a) and S2 (Figure 8b). As expected, the environmental impact due to CFCs (S1) is considerably greater than that related to the presence of HFCs (S2), both in terms of the GWP (on average 1134 for S1 and  $316 \text{ kgCO}_2\text{eq/m}^2$  for S2) and the ODP ( $243 \times 10^{-3}$  for S1 and  $0 \text{ kgCFC-11eq/m}^2$  for

S2). This is due to the higher environmental impact of CFCs with respect to HFCs. These quantities are characterized by quasi-Gaussian distributions with a non-negligible level of uncertainty (the CoV equal to 35% in all cases).

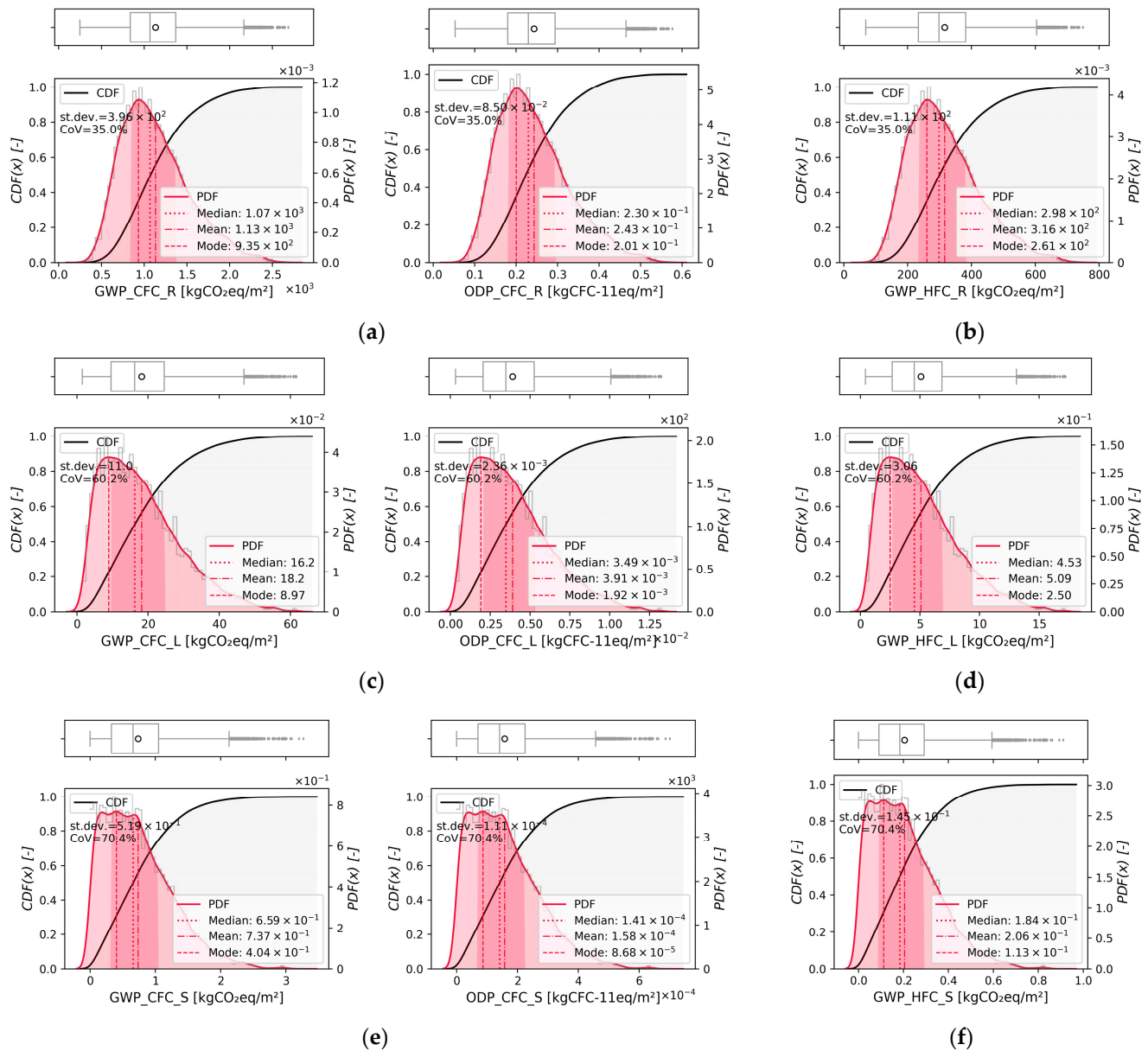


**Figure 8.** PDFs, CDFs, and box-whisker plots for the GWP and the ODP due to: residual content  $R_{tot}$  for: (a) S1 scenario; (b) S2 scenario. Operating annual losses  $L_{tot}$  for: (c) S1 scenario; (d) S2 scenario. Expected annual impact due to the occurrence of seismic events,  $S$ , for: (e) S1 scenario; (f) S2 scenario.

A direct comparison of these values with the annual impact for heat production (Figure 7) can be made, but it should be kept in mind that  $R_{tot}$  is emitted all at once just in case of the occurrence of an extreme seismic event. In this case, the residual banks may cause significantly greater impacts than those caused by annual energy consumption and, in particular, between 60 (S1) and 17 (S2) times the annual environmental impact due to heat production in terms of the GWP. For the ODP, the comparison is more trivial, especially for S1, as the heat production causes almost zero impact.



### 3.2.3. Expected Annual Impacts

Figure 8c,d report the impacts due to the total annual operational leakage of  $L_{tot}$  (i.e., the sum of  $L_I$  and  $L_{AC}$ ) in the S1 and S2 scenarios, respectively. For the sake of brevity, the annual impacts related to the individual  $L_I$  and  $L_{AC}$  are not reported due to the quite null share of  $L_{AC}$  on  $L_{tot}$  for the specific case study (see Figure 3). Therefore,  $L_{tot}$  can be considered to be representative of  $L_I$  impacts.

The PDFs are characterized by quasi-Gaussian shapes with average values of 18.23 (S1) and 5.08 (S2)  $\text{kgCO}_2\text{eq}/\text{m}^2$  and  $3.91 \times 10^{-3}$   $\text{kgCFC-11eq}/\text{m}^2$  (S1). The CoVs are equal to 60% for all the considered distributions, mainly caused by the high uncertainty in the leakage rate for the insulation materials (see Table 1).

If these average values are compared with those due to the annual heat production (Figure 7), it is possible to observe that, in terms of the GWP, the impacts due to  $L_{tot}$  banks are on average between 100 (S1) and 11% (S2) of those due to the annual heat production. In terms of the ODP, the comparison is more trivial, since the ODP due to heat production is null.

As a result, the removal and correct disposal of CFC/HFC banks can constitute, where technically feasible, significant environmental impact savings, even higher than that obtainable from energy retrofit measures.

Finally, Figure 8e,f report the expected annual impacts due to  $S_{tot}$ . The distributions are, in this case, characterized by negligible average values equal to 0.74 (S1) and 0.21 (S2)  $\text{kgCO}_2\text{eq}/\text{m}^2$  and  $0.16 \times 10^{-3}$  (S1)  $\text{kgCFC-11eq}/\text{m}^2$  with the CoV equal to 70% in all cases. These values are, on average, an order of magnitude lower than those related to the annual heat production and  $L_{tot}$  and, in particular, between 15 (S1) and 4% (S2) of the GWP due to the annual heat production.

### 3.2.4. Sensitivity Analysis

Figure 9 shows the results of the SA in terms of the  $S_T$  and  $S_I$  sensitivity indexes related to the annual GWP. Similar results are obtained for the ODP, and thus are not reported here for the sake of brevity. As expected, the variance of the parameters directly correlated to  $L_I$  has the greatest impact on the uncertainty of the result (higher  $S_T$  and  $S_I$ ). In order of importance, the parameters with high sensitivity indexes are  $l_I$ ,  $c_I$ , and  $\rho$ . This is because leakage from insulation material is the greater source of emission for the considered case study but also the most uncertain one, having a significant impact on the total annual GWP and variability. Therefore, knowledge of these parameters can then be important in the environmental assessment of a building.

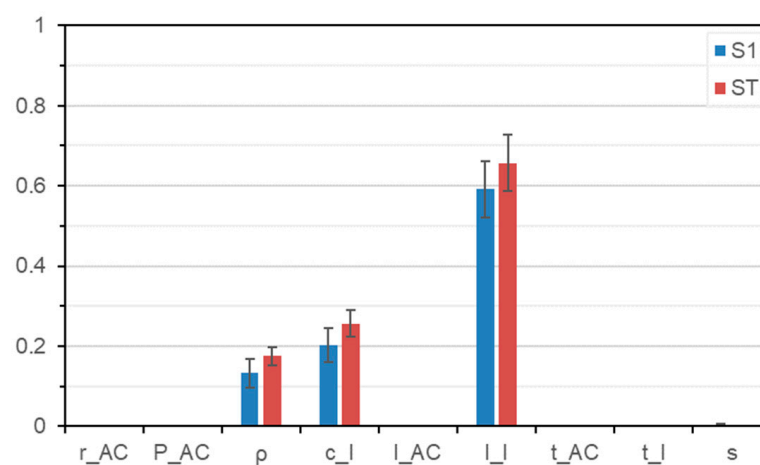


**Figure 9.** First-order ( $S_I$ ) and total-order ( $S_T$ ) sensitivity indexes for the expected annual impacts. Error bars represent the indexes' confidence intervals (with a confidence level of 95%).

### 3.3. Comparison of Environmental Retrofit Strategies

In this subsection, the LCA results related to the two iso performance environmental retrofit strategies described in Section 2.2.2, see Figure 1, are reported. The results of the stochastic LCA in terms of the ODP for the two solutions and S1 are reported in Figure 10, focusing on the relevant stages for each solution, i.e., the B1 stage for A-S1 (solution A, scenario 1) and the A5 stage for B-S1 (solution B, scenario 1). All other stages are characterized by a very low ODP, and then not reported for the sake of brevity. As expected, the two solutions differ by one order of magnitude, with higher results for A-S1. Thus, B-S1 can provide a consistent saving of ODP if employed, equal to, on average, about  $117 \times 10^{-3} \text{ kgCFC-11eq/m}^2$  for the considered case study. Differently, if HFCs are present (S2), the two solutions (A-S2 and B-S2) have an equal and null environmental impact in terms of the ODP.

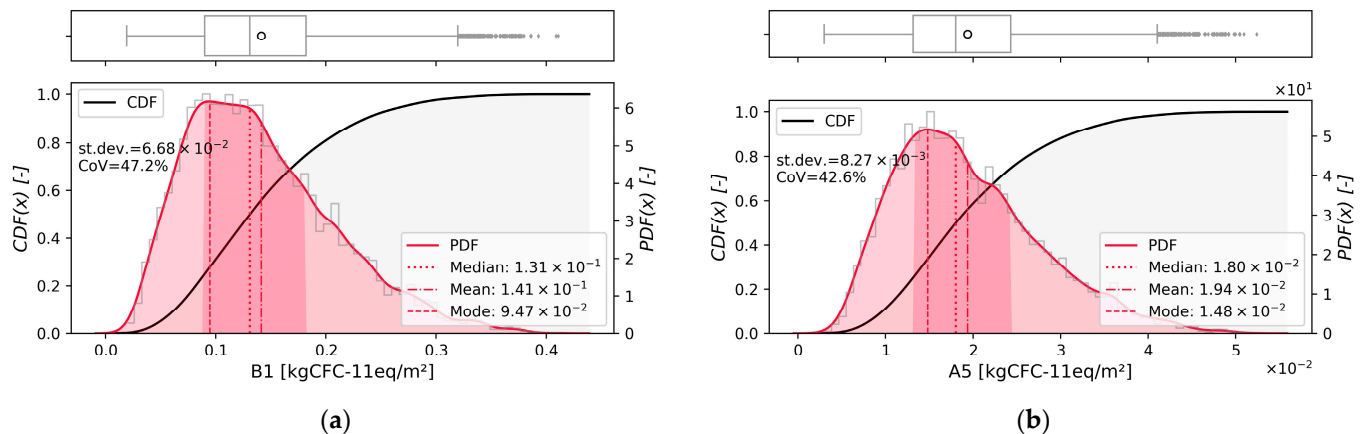


**Figure 10.** PDFs, CDFs, and box-whisker plots for the LCA results in terms of the main ODP impacts for: (a) Existing building and A-S1; (b) B-S1.

Regarding the GWP, Figure 11 reports the impacts related to heat production (B6) in pre- and post-retrofit scenarios. As can be seen, the energy retrofit can reduce, on average, the GWP of B6 about  $276 \text{ kgCO}_2\text{eq/m}^2$ . Concerning the other stages, Figure 12 reports the results related to A-S1 and B-S1 (Figure 12a and 12b, respectively). For the sake of brevity and conciseness, only the results related to A1–A3, A5, and B1 stages are reported, while EoL results (C1–C4) are not reported since they are negligible if compared to other stages. Similarly, Figure 13 reports the GWP related to A-S2 and B-S2. In this case, only the life cycle stages that differ from A-S1 and B-S1 are reported in this case, i.e., the B1 and A5 stages, respectively, since other results are those reported in Figure 12.

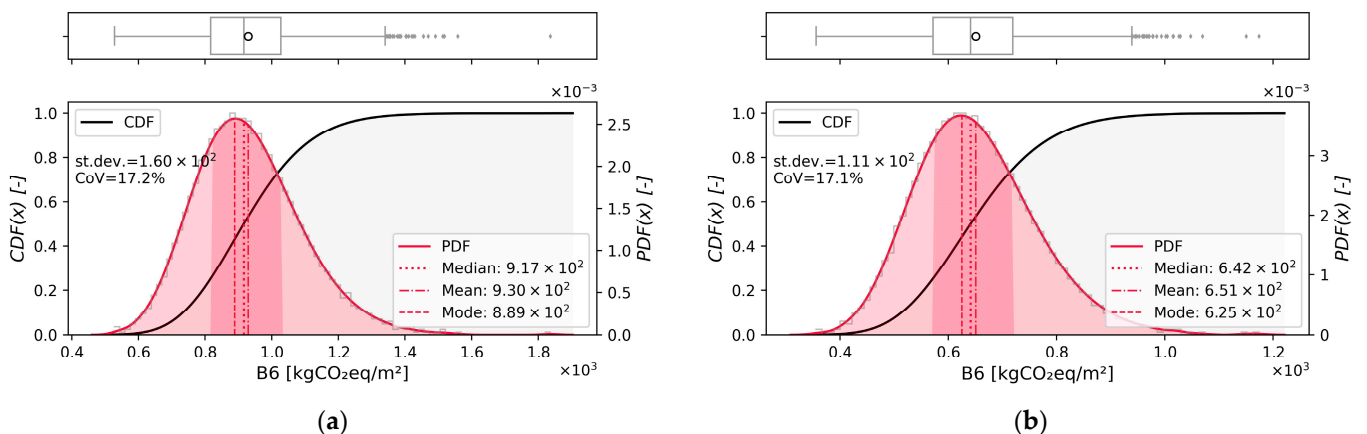


**Figure 11.** PDFs, CDFs, and box-whisker plots for the GWP due to heat production (B6) in: (a) the pre-retrofit scenario; (b) the post-retrofit scenario.

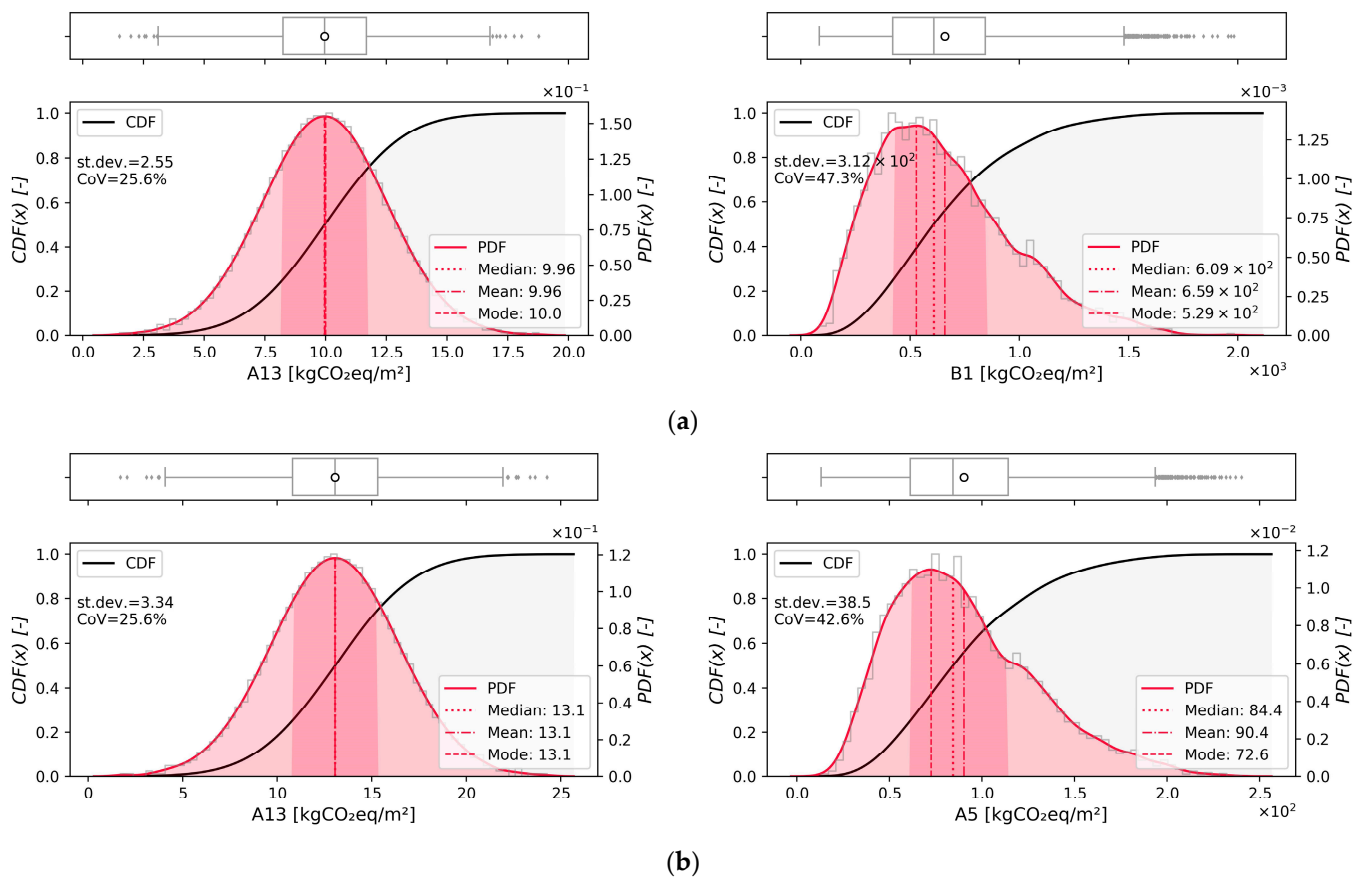


**Figure 12.** PDFs, CDFs, and box-whisker plots for the GWP related to relevant stages for: (a) A-S1; (b) B-S1. The EoL and A5 results are not reported, since they are negligible and equal to zero, respectively.

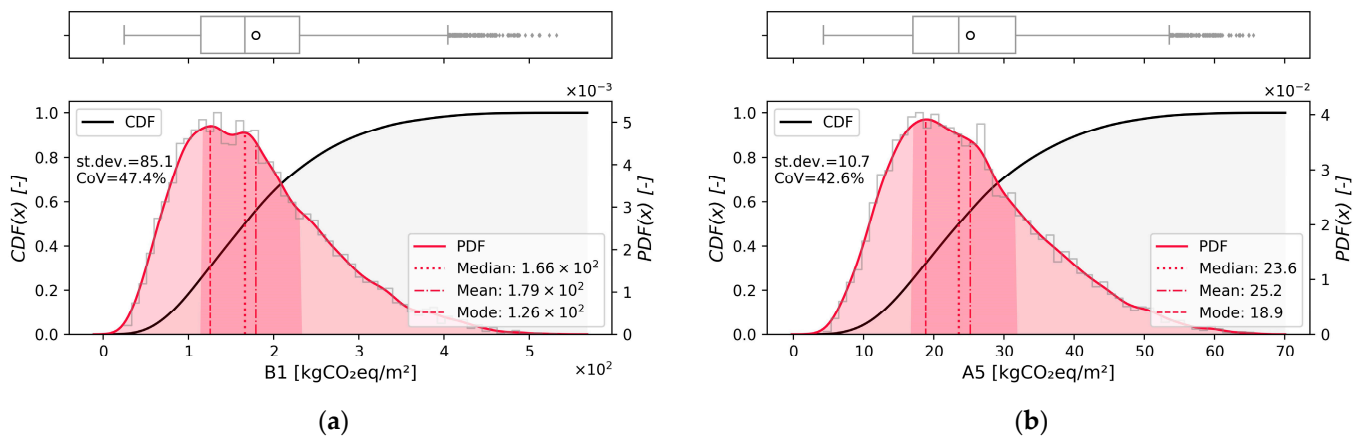


**Figure 13.** PDFs, CDFs, and box-whisker plots for the GWP related to the relevant stages for: (a) A-S2; (b) B-S2. In the latter case, only the B1 stage is reported, since it is the only one that differs from A-S1. The EoL and B1 results are not reported, since they are negligible and equal to zero, respectively.

One can see from Figure 12 that the two production stages are quite similar due to the similar quantity of materials involved in the retrofit measure (slightly higher for B-S1). Conversely, the B1 and A5 stages, for A-S1 and B-S1, respectively, are quite different, with B1 consistently higher than A5, by one order of magnitude. A similar result can be observed for A-S2 and B-S2 in Figure 13. As a result, with respect to A, B allows a noteworthy additional savings in terms of the GWP in all cases (on average 569 kgCO<sub>2</sub>eq/m<sup>2</sup> for

S1 and 151 kgCO<sub>2</sub>eq/m<sup>2</sup> for S2) even higher, for S1, than that achievable through the implementation of the energy retrofit measures (on average 276 kgCO<sub>2</sub>eq/m<sup>2</sup>).

Finally, in Figure 14a,b, the results of the sensitivity analyses related to the total GWP are reported for A-S1 and A-S2, respectively. The results for B-S1 and B-S2 are not reported, since all the total indexes are almost zero in this case except for GWP<sub>HP</sub> (which is then equal to almost 1). This is due to the high share of B6 on the total GWP for these latter cases.

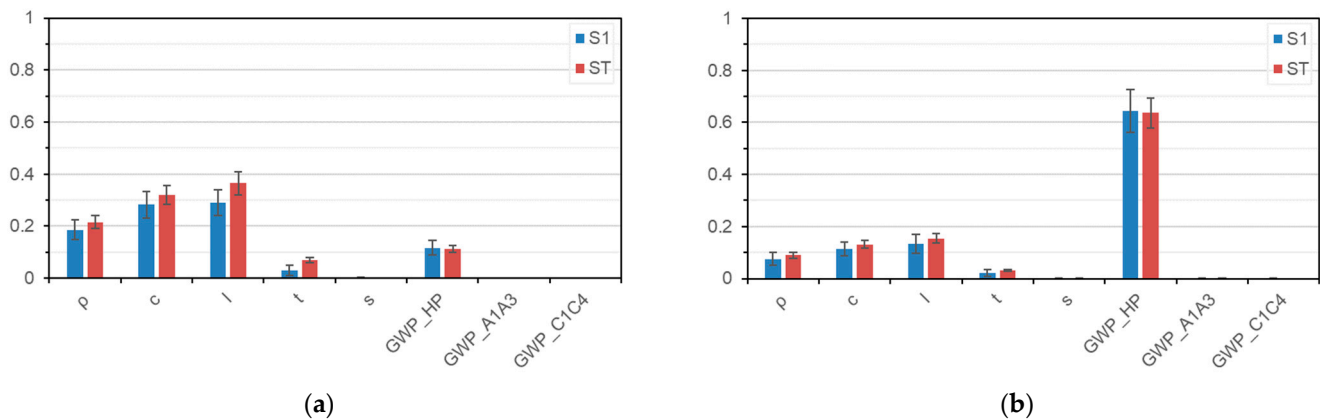


**Figure 14.** First-order ( $S_1$ ) and total-order ( $S_T$ ) sensitivity indexes for the total GWP impacts for: (a) A-S1; (b) A-S2. Error bars represent the indexes' confidence intervals (with a confidence level of 95%).

Again, except for GWP<sub>HP</sub>, whose  $S_T$  and  $S_1$  increase with an increase of the share of B6 in the total GWP (then, the indexes are higher in A-S2 than A-S1), the variance of the parameters directly correlated to  $l_1$  (which is the highest source of emission) has the highest  $S_T$  and  $S_1$ , and then the greatest impact on the output variance. In order of importance, the parameters with the highest sensitivity indexes are  $l_1$ ,  $c_1$ , and  $\rho$ . Therefore, this means that the knowledge of these parameters can be important in estimating the amount of CFC/HFC emissions in an LCA of a building. Contrariwise, other input variables have a quite negligible impact on the variance of the results.

#### 4. Conclusions

In this study, a comparative LCA was carried out to quantify the environmental impact of CFC/HFC banks in existing buildings and to evaluate the profitability of their removal and disposal as a potential environmental retrofit solution sustainable.

To achieve this aim, an analytical tool specifically developed in the literature was used and applied to a real case study (building archetype) [18,29], also extending it through uncertainty and sensitivity analysis to increase the results' reliability and to cope with the scarcity of data. The main findings of this study are summarized as follows:

- The largest CFC/HFC banks for the selected building archetypes are related to the thermal insulation foam ( $C_I$ ), which is, on average, 5.6 times higher than that contained in AC systems (on average 281 and 50 g/m<sup>2</sup>, respectively).
- $C_I$  is also responsible for the highest annual operational leakage of fluorocarbons into the environment, being about two orders of magnitude higher than that due to AC system banks (on average 3.43 and 0.05 g/m<sup>2</sup>, respectively).
- The fluorocarbons emitted annually due to seismic risk can vary between 0 and 0.13% of the total content (on average), mainly depending on the period and site of construction. In absolute terms, and for the specific buildings, this content is equal to 0.13 and 0.03 g/m<sup>2</sup>, and then quite negligible if compared to the annual CFC/HFC leakage from insulation (3.42 g/m<sup>2</sup>).
- In terms of the GWP, the annual impacts due to operation leakage are, on average, between 100 (CFCs) and 11% (HFCs) of the annual impact due to heat production

(about 18 kgCO<sub>2</sub>eq/m<sup>2</sup>). In terms of ODP, the comparison is more trivial, since the ODP due to heat production is null, while for CFCs it is four orders of magnitude higher ( $3.91 \times 10^{-3}$  kgCFC-11eq/m<sup>2</sup>).

- Concerning the comparative LCA, an ETICS-based retrofit intervention concerning the disposal of the existing the ETICS layer can provide a noteworthy additional GWP and ODP savings if compared to the simple superposition of a new ETICS layer. In the case of HFC banks, the additional reduction is related to the GWP only, and equal to 151 kgCO<sub>2</sub>eq/m<sup>2</sup>. In the case of CFCs, this reduction is higher, and, on average, equal to  $117 \times 10^{-3}$  kgCFC-11eq/m<sup>2</sup> for the ODP and 569 kgCO<sub>2</sub>eq/m<sup>2</sup> for the GWP. The latter saving is even higher than that achievable thanks to the energy saving in the use phase (on average 276 kgCO<sub>2</sub>eq/m<sup>2</sup>).
- Finally, the parameters with the highest impact on the annual GWP and ODP (highest sensitivity indexes) are those related to the estimation of the annual operational leakage from insulation, due to the high bank size and parameter uncertainty with respect to the other parameters. These parameters should be better investigated to have a more precise estimation of the environmental impacts of CFC/HFC banks on a building ecoprofile.

In conclusion, the removal of CFC/HFC banks from existing buildings can constitute a potential solution to reduce the environmental impacts of existing buildings. Moreover, CFC/HFC banks should not be neglected in LCA studies of buildings due to their significant impact on the building ecoprofile.

The main limitation of this study lies in the economic and technical constraints. Indeed, the replacement of fluorocarbon-containing products in an existing building may require a major refurbishment and huge financial outlay. Therefore, the application of the described approach for an environmental retrofit could be limited in the number of applicable cases.

Further developments should cover the economic feasibility of this solution, the possible limitations of the current building codes, and the possibility to integrate this solution into the prescriptions for energy retrofits. Moreover, while the sources of HFC/CFC banks considered in this study are limited, the same procedure can be applied to other old construction materials with similar or different harmful contents. Future studies could also investigate the existence and relevant size of HFC/CFC banks in other construction materials, such as old foam insulation in service pipelines.

**Author Contributions:** Conceptualization, G.M. and R.A.; Methodology, G.M. and R.D.F.; Software, G.M.; Validation, G.M. and R.D.F.; Formal analysis, G.M. and R.D.F.; Investigation, G.M. and R.D.F.; Resources, G.M.; Data curation, G.M.; Writing—original draft preparation, G.M. and R.D.F.; Writing—review and editing, G.M., R.D.F., R.A., O.S.B. and R.D.M.; Visualization, G.M.; Supervision, G.M., R.A. and R.D.M.; Project Administration, G.M. All authors have read and agreed to the published version of the manuscript.

**Funding:** This research received no external funding.

**Data Availability Statement:** The data presented in this study and the simulation code are available on request from the corresponding author.

**Acknowledgments:** The first, third, fourth, and last authors acknowledge the Italian Ministry of Education, Universities and Research (MUR) in the framework of the project DICAM-EXC (Departments of Excellence 2023–2027, grant L232/2016). The second author was supported by Habitech—Distretto Tecnologico Trentino S.c.a.r.l. Società Benefit with a research grant named in memory of Eng. Gianni Lazzari.

**Conflicts of Interest:** The authors declare no conflict of interest.



## References

1. Global Alliance for Buildings and Construction, International Energy Agency and the United Nations Environment Programme. 2019 Global Status Report for Buildings and Construction. 2019. Available online: <https://www.iea.org/reports/global-status-report-for-buildings-and-construction-2019> (accessed on 10 January 2023).
2. Pörtner, H.O.; Roberts, D.C.; Adams, H. *Climate Change 2022—Impacts, Adaptation and Vulnerability—Summary for Policymakers*; Cambridge University Press: Cambridge, UK; New York, NY, USA, 2022; ISBN 978-92-9169-159-3.
3. IEA Net Zero by 2050—Analysis—IEA. Available online: <https://www.iea.org/reports/net-zero-by-2050> (accessed on 10 January 2023).
4. Asif, M.; Muneer, T. Energy Supply, Its Demand and Security Issues for Developed and Emerging Economies. *Renew. Sustain. Energy Rev.* **2007**, *11*, 1388–1413. [\[CrossRef\]](#)
5. Economidou, M.; Atanasiu, B.; Staniaszek, D.; Maio, J.; Nolte, I.; Rapf, O.; Laustsen, J.; Ruyssevelt, P.; Strong, D.; Zinetti, S. *Europe's Buildings under the Microscope—A Country-by-Country Review of the Energy Performance of Buildings*; Buildings Performance Institute Europe: Brussels, Belgium, 2011; ISBN 978-94-91143-01-4.
6. IEA European Union 2020—Energy Policy Review. Available online: <https://www.iea.org/reports/european-union-2020> (accessed on 21 February 2023).
7. Finkelman, R.B.; Wolfe, A.; Hendryx, M.S. The Future Environmental and Health Impacts of Coal. *Energy Geosci.* **2021**, *2*, 99–112. [\[CrossRef\]](#)
8. von der Leyen, U. *A Union That Strives for More: My Agenda for Europe*; Political Guidelines for the Next European Commission; European Commission: Brussels, Belgium, 2019.
9. European Commission. *A Clear Planet for All—A European Strategic Long-Term Vision for a Prosperous, Modern, Competitive and Climate Neutral Economy*; COM (2018) 773 Final; European Commission: Brussels, Belgium, 2018.
10. European Commission. *The European Green Deal—Communication from the Commission to the European Parliament, the European Council, the Council, the European Economic and Social Committee and the Committee of the Regions*; European Commission: Brussels, Belgium, 2019.
11. Dascalaki, E.G.; Argiropoulou, P.A.; Balaras, C.A.; Droutsas, K.G.; Kontoyiannidis, S. Benchmarks for Embodied and Operational Energy Assessment of Hellenic Single-Family Houses. *Energies* **2020**, *13*, 4384. [\[CrossRef\]](#)
12. Chastas, P.; Theodosiou, T.; Kontoleon, K.J.; Bikas, D. The Effect of Embodied Impact on the Cost-Optimal Levels of Nearly Zero Energy Buildings: A Case Study of a Residential Building in Thessaloniki, Greece. *Energies* **2017**, *10*, 740. [\[CrossRef\]](#)
13. Hu, M. A Building Life-Cycle Embodied Performance Index—The Relationship between Embodied Energy, Embodied Carbon and Environmental Impact. *Energies* **2020**, *13*, 1905. [\[CrossRef\]](#)
14. Yu, F.; Feng, W.; Leng, J.; Wang, Y.; Bai, Y. Review of the U.S. Policies, Codes, and Standards of Zero-Carbon Buildings. *Buildings* **2022**, *12*, 2060. [\[CrossRef\]](#)
15. Castro, P.J.; Araújo, J.M.M.; Martinho, G.; Pereiro, A.B. Waste Management Strategies to Mitigate the Effects of Fluorinated Greenhouse Gases on Climate Change. *Appl. Sci.* **2021**, *11*, 4367. [\[CrossRef\]](#)
16. Scheutz, C.; Fredenslund, A.M.; Nedenskov, J.; Kjeldsen, P. Release and Fate of Fluorocarbons in a Shredder Residue Landfill Cell: 2. Field Investigations. *Waste Manag.* **2010**, *30*, 2163–2169. [\[CrossRef\]](#)
17. Lickley, M.; Solomon, S.; Fletcher, S.; Velders, G.J.M.; Daniel, J.; Rigby, M.; Montzka, S.A.; Kuijpers, L.J.M.; Stone, K. Quantifying Contributions of Chlorofluorocarbon Banks to Emissions and Impacts on the Ozone Layer and Climate. *Nat. Commun.* **2020**, *11*, 1380. [\[CrossRef\]](#)
18. Di Filippo, R.; Bursi, O.S.; di Maggio, R. Global Warming and Ozone Depletion Potentials Caused by Emissions from HFC and CFC Banks Due to Structural Damage. *Energy Build.* **2022**, *273*, 112385. [\[CrossRef\]](#)
19. U.S. Department of State, Office of Environmental Quality. Montreal Protocol on Substances that Deplete the Ozone Layer Final Act 1987. *J. Environ. Law* **1989**, *1*, 128–136. [\[CrossRef\]](#)
20. Newman, P.A.; Oman, L.D.; Douglass, A.R.; Fleming, E.L.; Frith, S.M.; Hurwitz, M.M.; Kawa, S.R.; Jackman, C.H.; Krotkov, N.A.; Nash, E.R.; et al. What Would Have Happened to the Ozone Layer If Chlorofluorocarbons (CFCs) Had Not Been Regulated? *Atmos. Chem. Phys.* **2009**, *9*, 2113–2128. [\[CrossRef\]](#)
21. Huang, J.; Mendoza, B.; Daniel, J.S.; Nielsen, C.J.; Rotsteyn, L.; Wild, O. Anthropogenic and Natural Radiative Forcing. In *Climate Change 2013: The Physical Science Basis. Contribution of Working Group I to the Fifth Assessment Report of the Intergovernmental Panel on Climate Change*; Stocker, T.F., Qin, D., Plattner, G.-K., Tignor, M., Allen, S.K., Boschung, J., Nauels, A., Xia, Y., Bex, V., Midgley, P.M., Eds.; Cambridge University Press: Cambridge, UK; New York, NY, USA, 2013; Volume 9781107057, pp. 659–740. [\[CrossRef\]](#)
22. Velders, G.J.M.; Fahey, D.W.; Daniel, J.S.; Andersen, S.O.; McFarland, M. Future Atmospheric Abundances and Climate Forcings from Scenarios of Global and Regional Hydrofluorocarbon (HFC) Emissions. *Atmos. Environ.* **2015**, *123*, 200–209. [\[CrossRef\]](#)
23. WMO (World Meteorological Organization). *Scientific Assessment of Ozone Depletion: 2018—Report No. 58*; WMO: Geneva, Switzerland, 2018; ISBN 978-1-73293-171-8.
24. Heath, E.A. Amendment to the Montreal Protocol on Substances That Deplete the Ozone Layer (Kigali Amendment). *Int. Leg. Mater.* **2017**, *56*, 193–205. [\[CrossRef\]](#)
25. Kjeldsen, P.; Jensen, M.H. Release of CFC-11 from Disposal of Polyurethane Foam Waste. *Environ. Sci. Technol.* **2001**, *35*, 3055–3063. [\[CrossRef\]](#)

26. Scheutz, C.; Fredenslund, A.M.; Kjeldsen, P.; Tant, M. Release of Fluorocarbons from Insulation Foam in Home Appliances during Shredding. *J. Air Waste Manag. Assoc.* **2007**, *57*, 1452–1460. [\[CrossRef\]](#)
27. Beshr, M.; Aute, V.; Abdelaziz, O.; Fricke, B.; Radermacher, R. Potential Emission Savings from Refrigeration and Air Conditioning Systems by Using Low GWP Refrigerants. *Int. J. Life Cycle Assess.* **2017**, *22*, 675–682. [\[CrossRef\]](#)
28. Llopis, R.; Calleja-Anta, D.; Maiorino, A.; Nebot-Andrés, L.; Sánchez, D.; Cabello, R. TEWI Analysis of a Stand-Alone Refrigeration System Using Low-GWP Fluids with Leakage Ratio Consideration. *Int. J. Refrig.* **2020**, *118*, 279–289. [\[CrossRef\]](#)
29. Di Filippo, R.; Bursi, O.S.; Ragazzi, M.; Ciucci, M. Natech Risk and the Impact of High-GWP Content Release on LCA of Industrial Components. *Process. Saf. Environ. Prot.* **2022**, *160*, 683–694. [\[CrossRef\]](#)
30. Flerlage, H.; Velders, G.J.M.; de Boer, J. A Review of Bottom-up and Top-down Emission Estimates of Hydrofluorocarbons (HFCs) in Different Parts of the World. *Chemosphere* **2021**, *283*, 131208. [\[CrossRef\]](#)
31. Montzka, S.A.; Dutton, G.S.; Yu, P.; Ray, E.; Portmann, R.W.; Daniel, J.S.; Kuijpers, L.; Hall, B.D.; Mondeel, D.; Siso, C.; et al. An Unexpected and Persistent Increase in Global Emissions of Ozone-Depleting CFC-11. *Nature* **2018**, *557*, 413–417. [\[CrossRef\]](#) [\[PubMed\]](#)
32. Ashford, P.; Clodic, D.; McCulloch, A.; Kuijpers, L. Emission Profiles from the Foam and Refrigeration Sectors Comparison with Atmospheric Concentrations. Part 2: Results and Discussion. *Int. J. Refrig.* **2004**, *27*, 701–716. [\[CrossRef\]](#)
33. Baldoni, E.; Coderoni, S.; Di Giuseppe, E.; D’Orazio, M.; Esposti, R.; Maracchini, G. A Software Tool for a Stochastic Life Cycle Assessment and Costing of Buildings’ Energy Efficiency Measures. *Sustainability* **2021**, *13*, 7975. [\[CrossRef\]](#)
34. Di Giuseppe, E.; D’Orazio, M.; Du, G.; Favi, C.; Lasvaux, S.; Maracchini, G.; Padey, P. A Stochastic Approach to LCA of Internal Insulation Solutions for Historic Buildings. *Sustainability* **2020**, *12*, 1535. [\[CrossRef\]](#)
35. Loga, T.; Stein, B.; Diefenbach, N. TABULA Building Typologies in 20 European Countries—Making Energy-Related Features of Residential Building Stocks Comparable. *Energy Build.* **2016**, *132*, 4–12. [\[CrossRef\]](#)
36. Decree of the President of the Republic. 26 August 1993, n. 412. GU N 242 14 Ottobre 1993. 1993. (In Italian). Available online: [https://www.bosettiegatti.eu/info/norme/statali/1993\\_0412.htm](https://www.bosettiegatti.eu/info/norme/statali/1993_0412.htm) (accessed on 10 January 2023).
37. Papst, I. *Banks and Emissions of CFC-11 and CFC-12: Country Data and Possible Consequences for Global Modelling*; Deutsche Gesellschaft für Internationale Zusammenarbeit (GIZ) GmbH: Eschborn, Germany, 2020.
38. Metz, B.; Kuijpers, L.; Solomon, S.; Andersen, S.O.; Davidson, O.R.; Meyer, L. *IPCC/TEAP Special Report Safeguarding the Ozone Layer and the Global Climate System: Issues Related to Hydrofluorocarbons and Perfluorocarbons*; Cambridge University Press: Cambridge, UK, 2005.
39. Ministero dello Sviluppo Economico. *Decreto Interministeriale 26.06.2015–Applicazione Delle Metodologie di Calcolo Delle Prestazioni Energetiche e Definizione Delle Prescrizioni e Dei Requisiti Minimi Degli Edifici*; Ministero dello Sviluppo Economico: Rome, Italy, 2015.
40. Casaburi, R.; Prato, F.; Vineis, D. *Manuale Pratico per la Progettazione Sostenibile*; Legislazione Tecnica: Lazio, Italy, 2016.
41. Grazieschi, G.; Asdrubali, F.; Thomas, G. Embodied Energy and Carbon of Building Insulating Materials: A Critical Review. *Clean. Environ. Syst.* **2021**, *2*, 100032. [\[CrossRef\]](#)
42. DM 26/06/2015; Requisiti Minimi. Schemi e Modalità di Riferimento per la Compilazione Della Relazione Tecnica di Progetto ai Fini Dell’applicazione Delle Prescrizioni e dei Requisiti Minimi di Prestazione Energetica Negli Edifici. 2015. Available online: <https://biblus.acca.it/download/decreto-requisiti-minimi-dm-26-giugno-2015/> (accessed on 10 January 2023). (In Italian)
43. D’Orazio, M.; Stipa, P.; Sabbatini, S.; Maracchini, G. Experimental Investigation on the Durability of a Novel Lightweight Prefabricated Reinforced-EPS Based Construction System. *Constr. Build. Mater.* **2020**, *252*, 119134. [\[CrossRef\]](#)
44. Poggi, F.; Macchi-Tejeda, H.; Leducq, D.; Bontemps, A. Refrigerant Charge in Refrigerating Systems and Strategies of Charge Reduction. *Int. J. Refrig.* **2008**, *31*, 353–370. [\[CrossRef\]](#)
45. Wall, B.J. CFCs in Foam Insulation: The Recovery Experience. In Proceedings of the ACEE 1994 Summer Study on Energy Efficiency in Buildings; 1994; pp. 269–276.
46. Vetter, A.A.J.; Ashford, P.K. *Developing a California Inventory for Ozone Depleting Substances (ODS) and Hydrofluorocarbon (HFC) Foam Banks and Emissions from Foams*; California Environmental Protection Agency: Sacramento, CA, USA, 2011.
47. Yazici, B.; Can, Z.S.; Calli, B. Prediction of Future Disposal of End-of-Life Refrigerators Containing CFC-11. *Waste Manag.* **2014**, *34*, 162–166. [\[CrossRef\]](#)
48. Maracchini, G.; Latini, A.; Di Giuseppe, E.; D’Orazio, M. Un Nuovo Strumento per Analisi Di Incertezza e Sensibilità Su Strategie Di Mitigazione Del Fenomeno Isola Di Calore Urbana. In Proceedings of the Colloqui.AT.e 2021–Ar.Tec. Conference, 8–11 September 2021; Sicignano, E., Ed.; EdicomEdizioni: Salerno, Italy, 2021.
49. Maracchini, G.; Bavarsad, F.S.; Di Giuseppe, E.; D’Orazio, M. Sensitivity and Uncertainty Analysis on Urban Heat Island Intensity Using the Local Climate Zone (LCZ) Schema: The Case Study of Athens. In Proceedings of the Sustainability in Energy and Buildings 2022, Split, Croatia, 14–16 September 2022; Littlewood, J., Howlett, R.J., Jain, L.C., Eds.; Springer Nature: Singapore, 2023; pp. 281–290.
50. Calm, J.M. Refrigerant Charge in Air-Conditioning Equipment with Selected Refrigerant Alternatives, Report JMC/AFEAS-9106C for the Alternative Fluorocarbons Environmental Acceptability Study. 1991. Available online: <http://jamesmcalm.com/pubs/Calm%20JM,%201991.%20Refrigerant%20Charge%20in%20Air-Conditioning%20Equipment%20with%20Selected%20Refrigerant%20Alternatives,%20report%20JMC-AFEAS-9106C,%20AFEAS,%20Washington,%20DC,%20USA.pdf> (accessed on 10 January 2023).

51. Bostock, D. Refrigerant Loss, System Efficiency and Reliability—A Global Perspective. In Proceedings of the Institute of Refrigeration Annual Conference, Colorado Springs, CO, USA, 17–20 March 2013.
52. Francis, C.; Maidment, G.; Davies, G. An Investigation of Refrigerant Leakage in Commercial Refrigeration. *Int. J. Refrig.* **2017**, *74*, 12–21. [\[CrossRef\]](#)
53. Simonen, K.; Huang, M.; Aicher, C.; Morris, P. Embodied Carbon as a Proxy for the Environmental Impact of Earthquake Damage Repair. *Energy Build.* **2018**, *164*, 131–139. [\[CrossRef\]](#)
54. Saito, T.; Fang, X.; Stohl, A.; Yokouchi, Y.; Zeng, J.; Fukuyama, Y.; Mukai, H. Extraordinary Halocarbon Emissions Initiated by the 2011 Tohoku Earthquake. *Geophys. Res. Lett.* **2015**, *42*, 2500–2507. [\[CrossRef\]](#)
55. Pan, C.; Wang, H.; Huang, S.; Zhang, H. The Great East Japan Earthquake and Tsunami Aftermath: Preliminary Assessment of Carbon Footprint of Housing Reconstruction. *Adv. Nat. Technol. Hazards Res.* **2014**, *35*, 435–450.
56. Maracchini, G.; Di Giuseppe, E.; Stazi, F.; D’Orazio, M. Approcci Probabilistici Alla Valutazione Dei Costi Globali Di Interventi Di Miglioramento Sismico Di Edifici. In *Colloqui.AT.e 2020—New Horizons for Sustainable Architecture*; Cascone, S.M., Margani, G., Sapienza, V., Eds.; EdicomEdizioni: Catania, Italia, 2020; pp. 1338–1354, ISBN 978-88-96386-94-1.
57. Cornell, C.A.; Krawinkler, H. Progress and Challenges in Seismic Performance Assessment. *PEER Cent. News* **2000**, *3*, 1–3.
58. ISO 14040:2006; Environmental Management—Life Cycle Assessment—Principles and Framework. ISO—International Organization for Standardization: Geneva, Switzerland, 2006. [\[CrossRef\]](#)
59. ISO 14044:2006; Environmental Management—Life Cycle Assessment—Requirements and Guidelines. ISO—International Standard Organization: Geneva, Switzerland, 2006.
60. EN 15804:2011; Sustainability of Construction Works—Environmental Product Declarations—Core Rules for the Product Category of Construction Products. CEN—European Committee for Standardization: Brussels, Belgium, 2011.
61. EN 15978:2011; Sustainability of Construction Works—Assessment of Environmental Performance of Buildings—Calculation Method. CEN—European Committee for Standardization: Brussels, Belgium, 2011; pp. 1–61.
62. de Bruijn, H.; van Duin, R.; Huijbregts, M.A.J.; Guinee, J.B.; Gorree, M.; Heijungs, R.; Huppes, G.; Kleijn, R.; de Koning, A.; van Oers, L.; et al. *Handbook on Life Cycle Assessment: An Operational Guide to the ISO Standards*; Springer: Dordrecht, The Netherlands, 2002; Volume 7, ISBN 978-1-4020-0228-1. [\[CrossRef\]](#)
63. Thibodeau, C.; Bataille, A.; Sié, M. Building Rehabilitation Life Cycle Assessment Methodology—State of the Art. *Renew. Sustain. Energy Rev.* **2019**, *103*, 408–422. [\[CrossRef\]](#)
64. Khasreen, M.M.M.; Banfill, P.F.G.F.G.; Menzies, G.F.F. Life-Cycle Assessment and the Environmental Impact of Buildings: A Review. *Sustainability* **2009**, *1*, 674–701. [\[CrossRef\]](#)
65. Frischknecht, R.; Jungbluth, N.; Althaus, H.-J.; Doka, G.; Dones, R.; Heck, T.; Hellweg, S.; Hirschier, R.; Nemecek, T.; Rebitzer, G.; et al. The Ecoinvent Database: Overview and Methodological Framework (7 Pp). *Int. J. Life Cycle Assess.* **2005**, *10*, 3–9. [\[CrossRef\]](#)
66. Pomponi, F.; D’Amico, B.; Moncaster, A. A Method to Facilitate Uncertainty Analysis in LCAs of Buildings. *Energies* **2017**, *10*, 524. [\[CrossRef\]](#)
67. Rivalin, L.; Stabat, P.; Marchio, D.; Caciolo, M.; Hopquin, F. A Comparison of Methods for Uncertainty and Sensitivity Analysis Applied to the Energy Performance of New Commercial Buildings. *Energy Build.* **2018**, *166*, 489–504. [\[CrossRef\]](#)
68. Meletti, C.; Montaldo, V.; Stucchi, M.; Martinelli, F. *Database Della Pericolosità Sismica MPS04*; Istituto Nazionale Di Geofisica e Vulcanologia (INGV): Milan, Italy, 2006. [\[CrossRef\]](#)

**Disclaimer/Publisher’s Note:** The statements, opinions and data contained in all publications are solely those of the individual author(s) and contributor(s) and not of MDPI and/or the editor(s). MDPI and/or the editor(s) disclaim responsibility for any injury to people or property resulting from any ideas, methods, instructions or products referred to in the content.